

THE OFFICIAL MAGAZINE OF THE OCEANOGRAPHY SOCIETY

Oceanography

CITATION

Schmitt, R.W., and A. Blair. 2015. A river of salt. *Oceanography* 28(1):40–45,
<http://dx.doi.org/10.5670/oceanog.2015.04>.

DOI

<http://dx.doi.org/10.5670/oceanog.2015.04>

COPYRIGHT

This article has been published in *Oceanography*, Volume 28, Number 1, a quarterly journal of The Oceanography Society. Copyright 2015 by The Oceanography Society. All rights reserved.

USAGE

Permission is granted to copy this article for use in teaching and research. Republication, systematic reproduction, or collective redistribution of any portion of this article by photocopy machine, reposting, or other means is permitted only with the approval of The Oceanography Society. Send all correspondence to: info@tos.org or The Oceanography Society, PO Box 1931, Rockville, MD 20849-1931, USA.

A River of Salt

By Raymond W. Schmitt and Austen Blair

ABSTRACT. Terrestrial rivers are a well-known part of the global water cycle, and there has been recent discussion of “atmospheric rivers” that transport vast quantities of moisture from the tropical ocean to mid-latitudes in transient weather systems. Complementary “salt rivers” within the ocean are an equally important part of the global water cycle. They help define the ocean’s methods of returning water to where it is needed to maintain sea level and the global water cycle. One part of the Salinity Processes in the Upper-ocean Regional Study (SPURS) focused on the North Atlantic surface salinity maximum, where high evaporation rates remove freshwater from the ocean surface and leave dissolved salts behind. Much of the effort is devoted to understanding how that salty water disperses through lateral and vertical mixing processes. One important exit path is simple advection within the general circulation, which in the central Atlantic means the wind-driven “Sverdrup” circulation. Evaporation results in high salinity within the flow, marking a subsurface salt river within the ocean. Here, we examine the river’s structure as revealed in the average salinity field of the North Atlantic. Mid-ocean salinity maxima provide a unique opportunity to use an isohaline control volume approach for analyzing the mixing processes that disperse the high-salinity plume.

INTRODUCTION

The ocean covers over 70% of Earth’s surface, so it is natural to expect that it dominates the global water cycle. It is also the planet’s principal water reservoir, with over 96% of the water not bound up in minerals (Schmitt, 1995). Indeed, there would not be a water cycle without the ocean! The terrestrial water cycle pales in comparison, with the flow of all rivers summing to less than 10% of the evaporation from the ocean’s surface (Schanze et al., 2010). Of course, civilization is

vitaly dependent on that 10% for agriculture, drinking water, cooling water, and transportation. With ongoing global change threatening to increase the intensity of droughts and the severity of floods, improving understanding of the large oceanic water cycle has become a high priority (Schmitt, 2008).

This issue of *Oceanography* highlights the use of salinity as an indicator of the water cycle’s signature in the ocean. Salt is left behind when water evaporates, thus increasing salinity. Similarly, the input

of freshwater by rainfall or river flows dilutes salt concentrations and decreases salinity. The patterns of salinity variability in the ocean have long been recognized as an excellent indicator of the structure of the global water cycle (Wüst, 1936). More recently, the observed long-term trends in ocean salinity, with salty regions getting saltier and fresh regions fresher, have been identified as important indicators of a changing global water cycle (Durack and Wijffels, 2010; Durack et al., 2012).

The Salinity Processes in the Upper-ocean Regional Study (SPURS) is designed to help oceanographers decipher the salinity code that the water cycle has left behind in the ocean. From the summer of 2012 to the fall of 2013, the first SPURS project focused on the salinity maximum of the North Atlantic (SPURS-1), the open ocean’s saltiest site, where evaporation is strong and precipitation rare (see *Oceanography* vol. 21, no. 1, 2008; <http://tos.org/oceanography/archive/21-1.html>). A suite of SPURS moorings complemented by a variety of profiling floats, underwater and wave gliders, salinity-sensing drifters, and ship-based measurements is allowing the diagnosis of the salinity balance at the site of the salinity maximum (Fararr et al.,

2015, and Dohan et al., 2015, both in this issue) as well as identification of various contributing processes such as eddies (Gordon et al., 2015 and Riser et al., 2015, both in this issue), fine-scale intrusions, (Shcherbina et al., 2015, in this issue) and rainfall (Yang et al., 2015, in this issue).

The second SPURS project will focus on a high precipitation area of the tropical Pacific, where salinities are lowered by rainfall (SPURS-2 Planning Group, 2015, in this issue), from the summer of 2016 to the summer of 2017. While it is obvious that these oceanic features indicate how the atmosphere moves water from place to place around the globe, they also suggest how the ocean must be responding. Indeed, there would be many meters per year of regional change in sea level if the ocean were not constantly redistributing the water lost or gained at the surface. Careful study of salinity patterns can reveal how the ocean does this. The fact that the salinity path is opposite the freshwater path is very helpful here (Wijffels et al., 1992). That is, high-salinity patches develop where water is leaving the ocean's surface, so while salt must be transported away from such salt sources, freshwater must be continually flowing into such regions (Gordon and Giulivi, 2014). Similarly, when rain dilutes the surface ocean, salt must flow into those regions to maintain the salinity while the freshwater flows out.

But how does the flow of salty water conspire to transport freshwater in the opposite direction? This apparent contradiction can be understood by appreciating that the portion of salt water that is fresh is given by a factor of $(1-S)$ times the density of salt water (ρ_s), where S is the salinity expressed as a fractional portion by weight. That is, 35 psu would be ~ 0.035 parts per part, so the freshwater content would be 96.5% of the salt water mass. (Practical salinity [psu] is used as a close approximation to absolute salinity as defined by Wright et al., 2011.) This relationship can be expressed as an equation: $\rho_{fw} = \rho_s(1-S)$. Multiplying the density by the water velocity gives

a mass flux estimate for water and salt. The minus sign tells us that freshwater flows will be opposite those of salinity (Wijffels et al., 1991). This idea will be useful for attempting to quantify the transports of salt and freshwater, but for now we will explore some of the structure of the North Atlantic salinity field using climatological data from the 2009 World Ocean Atlas.

THE NORTH ATLANTIC SALINITY MAXIMUM

A good starting point for exploring the salinity field is to observe the similarity between surface salinity and evaporation minus precipitation (E-P) for the North Atlantic. Figure 1 shows estimates of their average structures from the net water flux estimates of Schanze et al. (2010) and surface salinity from the 2009 World Ocean Atlas climatology.

While it may be obvious that evaporation is necessary to increase ocean salinities, and Ekman convergences must determine the salinity maximum's position (O'Connor et al., 2005; Gordon and Giulivi, 2014), there is much to be learned about the mixing and advective processes that disperse this high-salinity

water. This was the focus of the SPURS-1 field program described by articles in this issue. This paper takes a look at subsurface propagation of high-salinity water and describes an initial effort to develop an alternative framework for quantifying the ocean mixing processes that disperse it.

Well-averaged salinity data sets have been constructed from millions of ship-based and robotic observations made over the past several decades. Although E-P patterns at the ocean surface must be generating the high salinity observed in mid-gyre, subsurface data are required to see what becomes of this salty water. Figure 2 shows a restricted portion of the salinity field: only that above 37 psu at both the surface and at 150 m depth. Two features are noteworthy: (1) the salty patch has moved to the west-southwest at depth, and (2) the highest salinities have been reduced.

Figure 3 shows that the saltiest water comes from the surface in mid-gyre and that salinity decreases as it spreads both vertically and laterally. While the subsurface maximum found to the southwest is certainly an advective feature, the general spread and attenuation must be

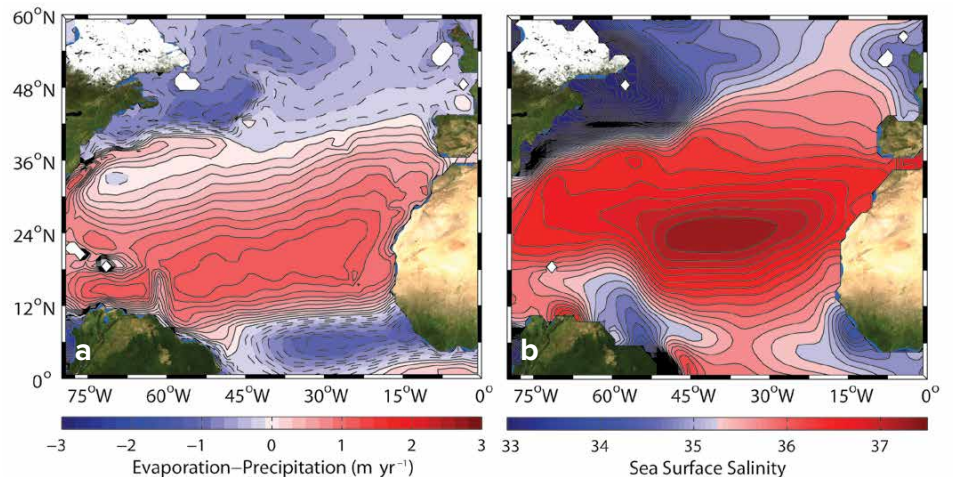


FIGURE 1. (a) Average evaporation minus precipitation (E-P) in meters per year from the data of Schanze et al. (2010). (b) Average surface salinity in the North Atlantic from 2009 World Ocean Atlas climatology. The mid-gyre salinity maximum is somewhat north of the strongest net water loss region due to Ekman transport, but they are clearly related. In general, areas of net water gain from precipitation and river flows are significantly fresher than regions of net water loss due to evaporation. Note the close correspondence between the zero line of E-P over the tropical Atlantic and the transition between forest and desert in West Africa. Clearly, the oceanic and terrestrial water cycles are closely connected.

due to mixing processes. An approach to quantifying those mixing processes will be discussed in the next section, but first we present one more view of our river of salt. This time the view is in three dimensions, from the perspective of someone high above South America (Figure 4). The sock shape of the 37.0 isohaline, with its toe kicking toward the Caribbean, is a striking picture of how the high salinity formed at the surface spreads within the ocean's interior. The atmosphere has transported water vapor from the middle to low latitudes, and the ocean must transport freshwater the opposite way. The “river of salt” can be thought of as draining an evaporative “salt shed,” which is the opposite of a water shed. This salt shed is manifested by the subsurface river of salt flowing to the southwest. In the North Atlantic, this high-salinity water is later carried poleward by the Gulf Stream, ultimately serving to compensate for global-scale transports of water vapor by the atmosphere (Wijffels et al., 1992).

A CONTROL VOLUME APPROACH TO THE SALINITY MAXIMUM BUDGET

One way to attempt to quantify the oceanic mixing processes that shape the river of salt is to use a “control volume” approach to budgeting. Given that a certain amount of freshwater is leaving or entering the ocean surface with the velocity $E-P$, we want to estimate how much

salt would be accumulating. A simple way to make this estimate is to construct a control volume box where the inputs through the boundaries are monitored (Figure 5). First, consider a very shallow box just below the ocean surface to assess the effect of the surface water flux on salinity. Take the average state of the sea surface to be level and ignore lateral variations because the scales of atmospheric variability are very large compared to our, say, one-meter-square box with a vanishingly small thickness. There is a certain flux of freshwater into or out of the ocean surface that must be compensated by a vertical flow through the bottom of the box, denoted by a velocity, w . This vertical velocity will have an average component and a fluctuating component denoted by $\bar{w} + w'$. This seawater velocity is composed of both freshwater and dissolved salts, and we know that only freshwater leaves (as E) or enters (as P) the ocean surface. Warren (2009) provides the details of such analysis, but the result is that over any averaging interval of interest, the net flux of salt into or out of the box given by $\rho_f(E-P)S$ must be compensated by an equal and opposite turbulent flux through the bottom of the box. Because only freshwater crosses the surface, the net transports of salt into the box must compensate over any interval with a constant salinity. Time-varying cases where the salinity may be changing can be considered as well. The upshot is that the expression for the vertical turbulent

salt flux ($\overline{w'S}$) just below the sea surface is $-(E-P)S$ averaged over any time interval of interest.

Now consider a much larger control volume and define it in a rather different way. This time, the volume considered is that part of the ocean enclosed by the sock-shaped outline of the average $S = 37.0$ isohaline shown in Figure 4. This is an artificial construct of course, because at any one point in time the actual shape of the $S = 37.0$ isohaline will be wildly complicated, with all sorts of dents and prominences caused by the eddies and waves of the ocean. And, unlike the simple box at the surface, the lateral flows and eddy transports through the sides of this volume must be considered in addition to the vertical fluxes because this volume has a substantial thickness. Figure 6 illustrates this concept.

The use of the climatological average $S = 37.0$ isohaline surface allows a simplification of the fluxes. That is, the average velocities across this surface will all be carrying the same salinity both in and out. So the average convergent velocities due to northward Ekman transport from the south and southward transport from the north that are compensated by Sverdrup transport down the “toe” of the sock will all be carrying the same average salinity. They will have a net convergence given by the total $E-P$ out of the surface area enclosed by the $S = 37.0$ curve of Figure 2a. Thus, the turbulent salt flux carried by lateral eddies and vertical turbulence will be given by the integral of $(E-P)S$ over that area. This term allows us to estimate the strength of those mixing processes. The use of an isohaline as a control surface is similar to the use of isotherms in tropical heat budgets by Niiler and Stevenson (1982) and more generally by Walin (1982), but in those applications, the isotherms contact the continents. For our salinity maximum, the isohaline control volume is entirely oceanic. Thus, the mid-gyre salinity maxima allow us to connect internal ocean mixing rates to surface fluxes.

A preliminary estimate of the

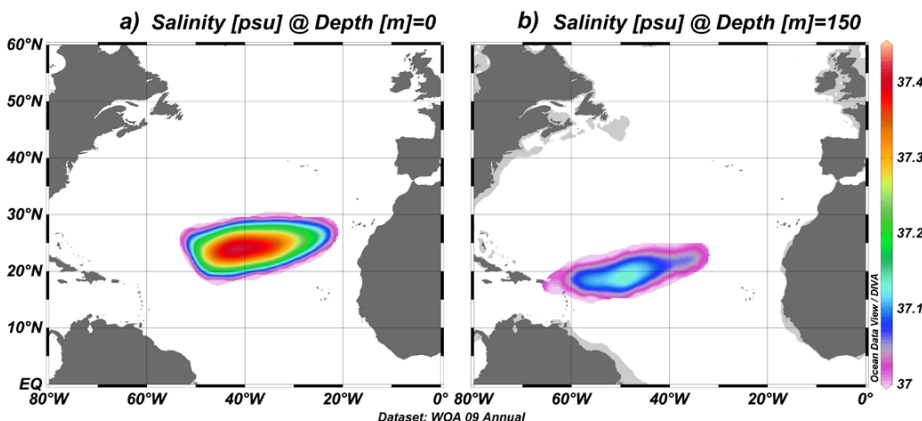


FIGURE 2. Salinities above 37 ppt (parts per thousand) at the surface (a) and at 150 m depth (b).

magnitude of the terms in such a balance for the Figure 5 salinity sock can be made from the present climatologies. Using the E–P estimates of Schanze et al. (2010) over about 20 years, we find that about 0.11 Sverdrups ($= 1.1 \times 10^5 \text{ m}^3 \text{ s}^{-1}$) is the long-term average water loss from the area enclosed by the 37.0 isohaline ($2.9 \times 10^6 \text{ km}^2$). Multiplication of E–P with the salinity within that area yields a net surface salt input of 3.9 psu-Sv to the control volume. This salt flux must be dispersed by the horizontal mixing processes acting on the sides of the salinity sock within the ocean and the vertical mixing processes acting over its bottom area. Such processes are often parameterized with “eddy diffusivities” acting on observed gradients. That is, the horizontal flux can be written as

$$F_{SH} = K_H \nabla_H S$$

where K_H is the diffusivity and $\nabla_H S$ is the horizontal salinity gradient. Similarly, the vertical flux is represented as

$$F_{SV} = K_V \frac{\partial S}{\partial Z}$$

In these equations, K_H and K_V represent horizontal and vertical eddy diffusivities that yield the horizontal and vertical salt fluxes F_{SH} and F_{SV} when multiplied by the horizontal gradient components

$$\frac{\partial S}{\partial X} + \frac{\partial S}{\partial Y} = \nabla_H S$$

and the vertical salt gradient

$$\frac{\partial S}{\partial Z}$$

Because the ocean is strongly stratified in Earth’s gravitational field, it takes a lot of energy to mix things vertically, but horizontal mixing occurs much more easily. Thus, lateral diffusivities are many times larger than vertical diffusivities. However, we also find that vertical gradients are much larger than horizontal gradients, so the net fluxes caused by each process can be comparable. In each case, such calculations are sensitive to the spatial scales over which gradients are estimated. Taking some preliminary estimates of gradients from the one-degree grid of climatological data, we find that

the surface input of salt can be accommodated by horizontal diffusivities of order $5,000 \text{ m}^2 \text{ s}^{-1}$ and vertical diffusivities between 1×10^{-5} and $1 \times 10^{-4} \text{ m}^2 \text{ s}^{-1}$, with 1/10 to 1/2 of the flux being contributed by the vertical processes. These estimates are very preliminary and apply over much larger scales than those sampled in the SPURS-1 study area. As progress is made with analysis of the SPURS data, a better understanding of the processes that contribute to both horizontal and vertical mixing processes will emerge. Of course, one of the limits of such analysis is the actual time variability in surface area and volume of the 37.0 isohaline. Eddies will certainly draw off enclosed blobs of $S > 37.0$ and temporarily expand its surface area. But

those are the mixing processes that must be quantified to construct a picture of how the mean structure of the 37.0 isohaline is maintained. As described by Gordon and Giulivi (2014), eddies must be a very significant supplier of freshwater to the salinity maximum region and a dispersal agent for salt. Mixing of the salinity variance to smaller scales is accomplished by internal waves and interleaving features such as those described by Shcherbina et al. (2015, in this issue).

The horizontal diffusivity estimated from the 2009 World Ocean Atlas climatology can be thought of as being driven by 50 km scale eddies with $\sim 10 \text{ cm s}^{-1}$ velocities, something very consistent what was observed during the SPURS-1 experiment. It is also roughly

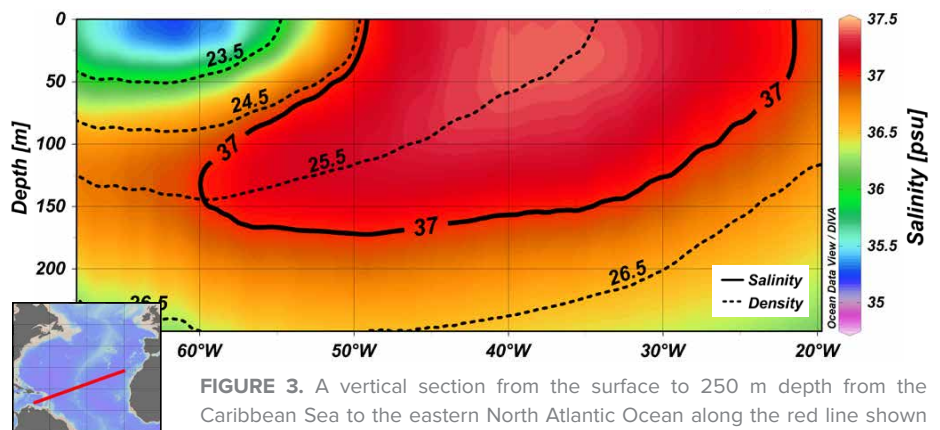


FIGURE 3. A vertical section from the surface to 250 m depth from the Caribbean Sea to the eastern North Atlantic Ocean along the red line shown in the lower left map, which was chosen to follow the southwest path of the subsurface expression of the salinity maximum. The climatological average profiles from the 2009 World Ocean Atlas were used to construct the section. The high-salinity core is seen to originate at the surface and is carried to the southwest by the wind-driven Sverdrup circulation, following the potential density surface of $1,025.5 \text{ Kg m}^{-3}$.

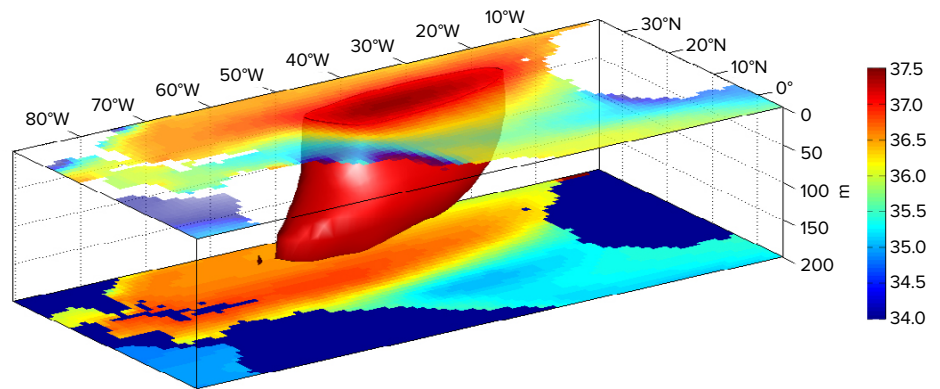


FIGURE 4. The three-dimensional shape of the 37.0 isohaline from a perspective over South America. The color scale indicates salinity at the surface and at 200 m depth. The continental and island land masses are transparent at the surface and blue at 200 m depth. The vertical exaggeration is about 20,000:1. The one-degree data of the 2009 World Ocean Atlas climatology were used.

comparable to eddy diffusivity estimates from the literature based on eddy statistics and drifter dispersion (Rypina et al., 2012; Abernathy and Marshall, 2013). In actuality, it is expected that the meridional and zonal diffusivities will be different. Such effects may be accessible with the surface drifter data obtained during the SPURS-1 field program, many of which were equipped with salinity sensors, so statistics of $\overline{v's'}$ may be accessible. The vertical salt diffusivity is thought to be due to turbulence caused by breaking internal waves and salt fingers acting on the unstable salt gradient of the region (Schmitt and Evans, 1978; Bauer and Siedler, 1988). Regional estimates of such diffusivities in the North Atlantic are between $1 \times 10^{-5} \text{ m}^2 \text{ s}^{-1}$ in a region to the east of the salt river (St. Laurent and Schmitt, 1999) and $1 \times 10^{-4} \text{ m}^2 \text{ s}^{-1}$ in the downstream end of the river of salt, where salt fingers become especially intense and form a strong thermohaline staircase (Schmitt et al., 2005). Indeed, it would appear that the salt sock is making a move to step down the thermohaline staircase. Preliminary analysis of SPURS-1 microstructure data does support the presence of salt fingers in the upper thermocline (L. St. Laurent, Woods Hole Oceanographic Institution, *pers. comm.*, 2014).

DISCUSSION

Attempts to estimate oceanic fluxes are always constrained by the limited data sets available to investigators. During SPURS-1, an extensive suite of instruments was deployed for a year. Though these data are providing new details on salinity processes, our analysis is inevitably limited by the duration and spatial extent of the available information. Here, we reached back into the climatology of the 2009 World Ocean Atlas to provide a big picture view of how the surface salinity maximum propagates into the ocean's interior. Mixing is obviously important because the salinity maximum decays away from the high values at the surface. Advection within the gyre's Sverdrup circulation is readily apparent in the southwesterly path of propagation. By using averaged data from several decades of ocean observations, a smooth and simplified picture of the structure of the river of salt is obtained. However, at any particular time, the actual structure of any one isohaline will be much more complex than presented in this smoothed climatological picture. SPURS scientists identified some of the complex processes in operation (Riser et al., 2015; Farrar et al., 2015; Shcherbina et al., 2015, all in this issue). Though it uses the concept of a mean isohaline surface, the budgeting

approach proposed here will help to place these processes into a larger-scale context and provide guidance on the magnitude of horizontal and vertical mixing rates. This ultimately will help to advance the development of ocean models. As Durack and Wijffels (2010) show, significant changes in salinity seem to be underway, with salty areas getting saltier and fresh areas getting fresher. Indeed, because most of the water cycle is over the ocean (Schmitt, 1995), observed long-term salinity trends are the best evidence we have that the water cycle is intensifying with global warming. Models do not yet describe these changes accurately (Durack et al., 2012), in part because we need to better understand oceanic mixing and advection. At stake is nothing less than our ability to predict the strength of water cycle intensification so that we can mitigate some of its consequences.

SUMMARY

The isohaline control volume approach promises to be a useful tool for understanding the mixing processes acting on the North Atlantic salinity maximum. Mid-ocean salt maxima are especially suited to such analysis because the volume enclosed by the isohaline is purely oceanic; there are no land boundaries to consider. Of course, many simplifying

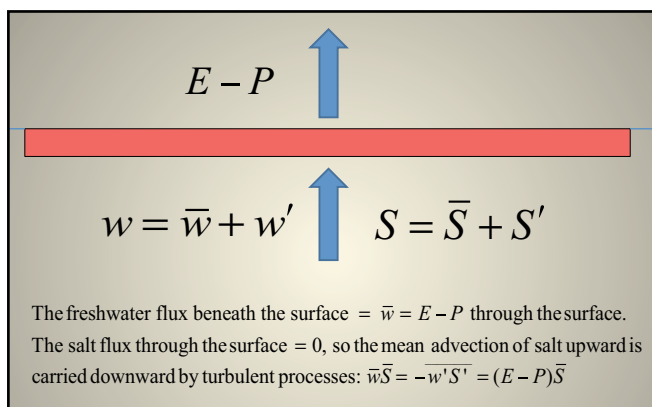


FIGURE 5. A small box at the ocean surface with water exchange with the atmosphere above. The salt carried into the box at depth by the net evaporation is compensated for by a turbulent transport of salt downward because the salinity does not change over the averaging interval of interest. This can be expressed as $\bar{w}\bar{S} = -\overline{w's'} = (E - P)\bar{S}$.

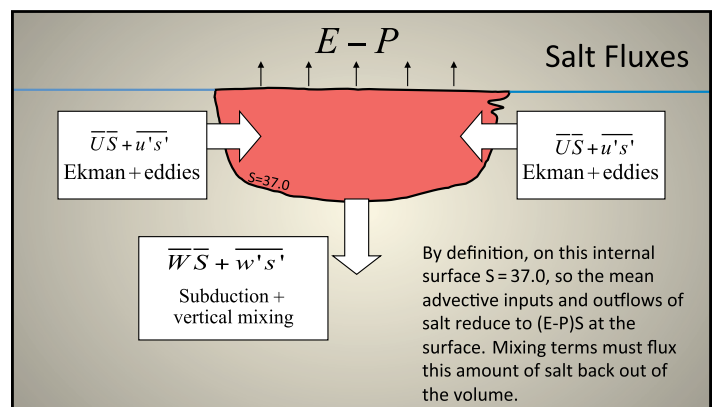



FIGURE 6. A control volume defined by the average shape of the 37.0 isohaline. Water and salt are pumped into the isohaline “sock” by Ekman convergences and taken out by surface fluxes ($E - P$), Sverdrup advection, subduction, and vertical and lateral mixing processes. The fact that all the mean advective flows into and out of the volume have the same salinity on this averaged isohaline surface means that the salt budget for the enclosed volume simplifies to a balance between salt input at the surface by net evaporation and dispersion by lateral and vertical mixing processes.

assumptions go into such an analysis. In truth, the seasonal and interannual variability of the isohaline volume and possible long-term trends will need to be considered. Nonetheless, the rich data set collected during SPURS-1 promises to elucidate some of the specifics of the lateral and vertical mixing mechanisms operating there. This control volume approach is an alternative to the single point salt balance examined in this special issue by Farrar et al. (2015) and promises a way to integrate many different types of data over a wider area.

Years ago, Worthington (1976) puzzled about the appearance and disappearance of the river of salt in two separate years and hypothesized that it was connected to the strength and position of the subtropical high pressure system over the Atlantic. At a basic level, he was most likely right, as the high dictates the strength of the trade winds that are driving both the evaporation and the Ekman convergence in the greater SPURS-1 region. But we are now in a much more data-rich era and can begin to quantify some of the salinity processes at work. As the predictions of global warming call for both an expansion of the subtropical high pressure systems (Li et al., 2012) and intensification of the water cycle (Held and Soden, 2006), it will be an interesting challenge for future oceanographers to document the evolution of the river of salt. 

ACKNOWLEDGEMENTS. RWS was supported by grants NNX12AF59G from NASA and 1129646 from the National Science Foundation. AB was supported by a Summer Student Fellowship from the Woods Hole Oceanographic Institution. Julian Schanze assisted with E–P data and Figure 1.

REFERENCES

Abernathy, R.P., and J. Marshall. 2013. Global surface eddy diffusivities derived from satellite altimetry. *Journal of Geophysical Research* 118:901–916, <http://dx.doi.org/10.1002/jgrc.20066>.

Bauer, E., and G. Siedler. 1988. The relative contributions of advection and isopycnal and diapycnal mixing below the subtropical salinity maximum. *Deep Sea Research Part A* 35:811–837, [http://dx.doi.org/10.1016/0198-0149\(88\)90032-5](http://dx.doi.org/10.1016/0198-0149(88)90032-5).

Dohan, K., H.-Y. Kao, and G.S.E. Lagerloef. 2015. The freshwater balance over the North Atlantic SPURS domain from Aquarius satellite salinity, OSCAR satellite surface currents, and some simplified approaches. *Oceanography* 28(1):86–95, <http://dx.doi.org/10.5670/oceanog.2015.07>.

Durack, P.J., and S.E. Wijffels. 2010. Fifty-year trends in global ocean salinities and their relationship to broad-scale warming. *Journal of Climate* 23:4,342–4,362, <http://dx.doi.org/10.1175/2010JCLI3377.1>.

Durack, P.J., S.E. Wijffels, and R.J. Matear. 2012. Ocean salinities reveal strong global water cycle intensification during 1950 to 2000. *Science* 336:455–458, <http://dx.doi.org/10.1126/science.1212222>.

Farrar, J.T., L. Rainville, A.J. Plueddemann, W.S. Kessler, C. Lee, B.A. Hodges, R.W. Schmitt, J.B. Edson, S.C. Riser, C.C. Eriksen, and D.M. Fratantoni. 2015. Salinity and temperature balances at the SPURS central mooring during fall and winter. *Oceanography* 28(1):56–65, <http://dx.doi.org/10.5670/oceanog.2015.06>.

Gordon, A.L., and C.F. Giulivi. 2014. Ocean eddy freshwater flux convergence into the North Atlantic subtropics. *Journal of Geophysical Research* 119:3,327–3,335, <http://dx.doi.org/10.1002/2013JC009596>.

Gordon, A.L., C.F. Giulivi, J. Busecke, and F.M. Bingham. 2015. Differences among subtropical surface salinity patterns. *Oceanography* 28(1):32–39, <http://dx.doi.org/10.5670/oceanog.2015.02>.

Held, I.M., and B.J. Soden. 2006. Robust responses of the hydrological cycle to global warming. *Journal of Climate* 19:5,686–5,699, <http://dx.doi.org/10.1175/JCLI3990.1>.

Li, W., L. Li, M. Ting, and Y. Liu. 2012. Intensification of Northern Hemisphere subtropical highs in a warming climate. *Nature Geoscience* 5:830–834, <http://dx.doi.org/10.1038/ngeo1590>.

Niiler, P., and J. Stevenson. 1982. The heat budget of tropical ocean warm-water pools. *Journal Marine Research* 40:465–480.

O'Connor, B.M., R.A. Fine, and D.B. Olson. 2005. A global comparison of subtropical under-water formation rates. *Deep Sea Research Part I* 52:1,569–1,590, <http://dx.doi.org/10.1016/j.dsr.2005.01.011>.

Riser, S.C., J. Anderson, A. Shcherbina, and E. D'Asaro. 2015. Variability in near-surface salinity from hours to decades in the eastern North Atlantic: The SPURS region. *Oceanography* 28(1):66–77, <http://dx.doi.org/10.5670/oceanog.2015.11>.

Rypina, I.I., I. Kamenkovich, P. Berloff, and L.J. Pratt. 2012. Eddy-induced particle dispersion in the near-surface North Atlantic. *Journal of Physical Oceanography* 42:2,206–2,228, <http://dx.doi.org/10.1175/JPO-D-11-0191.1>.

Schanze, J.J., R.W. Schmitt, and L.L. Yu. 2010. The global oceanic freshwater cycle: A state-of-the-art quantification. *Journal of Marine Research* 68:569–595, <http://dx.doi.org/10.1357/002224010794657164>.

Schmitt, R.W. 1995. The ocean component of the global water cycle. *Reviews of Geophysics* 33(S2):1,395–1,409, <http://dx.doi.org/10.1029/95RG00184>.

Schmitt, R.W. 2008. Salinity and the global water cycle. *Oceanography* 21(1):12–19, <http://dx.doi.org/10.5670/oceanog.2008.63>.

Schmitt, R.W., and D.L. Evans. 1978. An estimate of the vertical mixing due to salt fingers based on observations in the North Atlantic Central Water. *Journal of Geophysical Research* 83(C6):2,913–2,919, <http://dx.doi.org/10.1029/JC083iC06p02913>.

Schmitt, R.W., J.R. Ledwell, E.T. Montgomery, K.L. Polzin, and J.M. Toole. 2005. Enhanced diapycnal mixing by salt fingers in the thermocline of the tropical Atlantic. *Science* 308:685–688, <http://dx.doi.org/10.1126/science.1108678>.

Shcherbina, A.Y., E.A. D'Asaro, S.C. Riser, and W.S. Kessler. 2015. Variability and interleaving of upper-ocean water masses surrounding the North Atlantic salinity maximum. *Oceanography* 28(1):106–113, <http://dx.doi.org/10.5670/oceanog.2015.12>.

SPURS-2 Planning Group. 2015. From salty to fresh—Salinity Processes in the Upper-ocean Regional Study-2 (SPURS-2): Diagnosing the physics of a rainfall-dominated salinity minimum. *Oceanography* 28(1):150–159, <http://dx.doi.org/10.5670/oceanog.2015.15>.

St. Laurent, L., and R.W. Schmitt. 1999. The contribution of salt fingers to vertical mixing in the North Atlantic Tracer Release Experiment. *Journal of Physical Oceanography* 29:1,404–1,424, [http://dx.doi.org/10.1175/1520-0485\(1999\)029<1404:TCOSFT>2.0.CO;2](http://dx.doi.org/10.1175/1520-0485(1999)029<1404:TCOSFT>2.0.CO;2).

Warren, B.A. 2009. Note on the vertical velocity and diffusive salt flux induced by evaporation and precipitation. *Journal of Physical Oceanography* 39:2,680–2,682, <http://dx.doi.org/10.1175/2009JPO4069.1>.

Walín, G. 1982. On the relation between sea-surface heat flow and thermal circulation in the ocean. *Tellus* 34:187–195, <http://dx.doi.org/10.1111/j.2153-3490.1982.tb01806.x>.

Wijffels, S.E., R.W. Schmitt, H.L. Bryden, and A. Stigebrandt. 1992. Response of freshwater by the oceans. *Journal of Physical Oceanography* 22:155–162, [http://dx.doi.org/10.1175/1520-0485\(1992\)022<0155:TFOBTO>2.0.CO;2](http://dx.doi.org/10.1175/1520-0485(1992)022<0155:TFOBTO>2.0.CO;2).

Worthington, L.V. 1976. *On the North Atlantic Circulation*. The Johns Hopkins Oceanographic Studies Number 6, Johns Hopkins University Press, Baltimore, MD, 110 pp.

Wright, D.G., R. Pawlowicz, T.J. McDougall, R. Feistel, and G.M. Marion. 2011. Absolute Salinity, “Density Salinity” and the Reference-Composition Salinity Scale: Present and future use in the seawater standard TEOS-10. *Ocean Science* 7(1):1–26, <http://dx.doi.org/10.5194/os-7-1-2011>.

Wüst, G. 1936. Oberflächensalzgehalt, Verdunstung und Niederschlag auf den Weltmeere. *Landerkundliche Forschung*, Festschrift Norbert Krebs, 347–349.

Yang, J., S.C. Riser, J.A. Nystuen, W.E. Asher, and A.T. Jessup. 2015. Regional rainfall measurements using the Passive Aquatic Listener during the SPURS field campaign. *Oceanography* 28(1):124–133, <http://dx.doi.org/10.5670/oceanog.2015.10>.

AUTHORS. Raymond W. Schmitt (rschmitt@whoi.edu) is Senior Scientist, Department of Physical Oceanography, Woods Hole Oceanographic Institution, Woods Hole, MA, USA. Austen Blair is Graduate Student Research Assistant, Graduate School of Oceanography, University of Rhode Island, Narragansett, RI, USA.

ARTICLE CITATION

Schmitt, R.W., and A. Blair. 2015. A river of salt. *Oceanography* 28(1):40–45, <http://dx.doi.org/10.5670/oceanog.2015.04>.